University of Groningen

Bacillus subtilis at near-zero specific growth rates

Overkamp, Wout

IMPORTANT NOTE: You are advised to consult the publisher's version (publisher's PDF) if you wish to cite from it. Please check the document version below.

Document Version
Publisher's PDF, also known as Version of record

Publication date:
2015

Link to publication in University of Groningen/UMCG research database

Citation for published version (APA):
Overkamp, W. (2015). *Bacillus subtilis at near-zero specific growth rates: adaptations to extreme caloric restriction*. University of Groningen.

Copyright
Other than for strictly personal use, it is not permitted to download or to forward/distribute the text or part of it without the consent of the author(s) and/or copyright holder(s), unless the work is under an open content license (like Creative Commons).

The publication may also be distributed here under the terms of Article 25fa of the Dutch Copyright Act, indicated by the "Taverne" license. More information can be found on the University of Groningen website: https://www.rug.nl/library/open-access/self-archiving-pure/taverne-amendment.

Take-down policy
If you believe that this document breaches copyright please contact us providing details, and we will remove access to the work immediately and investigate your claim.

Downloaded from the University of Groningen/UMCG research database (Pure): http://www.rug.nl/research/portal. For technical reasons the number of authors shown on this cover page is limited to 10 maximum.

Download date: 21-06-2022

6

Single-cell analysis during *Bacillus subtilis′* diauxic shift

Wout Overkamp, Renske Veenendaal, Reto D. Zwahlen, Oscar P. Kuipers

Abstract

When bacteria encounter environments with two carbohydrates, the preferred carbon source, usually glucose, is utilized first and then the second one. The resulting two growth phases are separated by the typical diauxic lag phase. This lag phase is classically explained as the time that cells need for biochemical adaptation to the second carbohydrate and assumes that all cells make this switch. *B. subtilis* is able to generate various phenotypes within an isogenic population. Is *B. subtilis'* metabolism also prone to this phenotypic variation? Using time-lapse microscopy we show that, in compliance with traditional views, genes for uptake and utilization of the second carbohydrate, e.g. ribose or cellobiose, are expressed during the lag phase in all cells, at the same point in time. However, the transcription of genes occurs at different rates in each cell, resulting in heterogeneity.

Introduction

Nutrient concentrations fluctuate over time in natural environments and bacteria employ various strategies to ensure survival and growth (Demoling et al., 2007; Koch, 1971). When multiple carbohydrates are present, not all are consumed simultaneously by the bacterial cells, but solely the one that allows the highest growth rate (Inada et al., 1996; Stülke and Hillen, 1999). The mechanism responsible for this is carbon catabolite repression (CCR; for more info see Chapter 1). After exhaustion of the preferred carbohydrate (in many cases glucose), cells switch to the second-preferred carbohydrate. This results in a biphasic growth pattern, so-called 'diauxie' (Monod, 1949). During the shift from one carbon source to another, a certain period exists during which the culture lacks apparent growth. This lag phase is classically explained as the time that cells need for biochemical adaptation to the new substrate (Stanier, 1951).

Traditionally, cells are considered to switch homogeneously to a second carbon source, with the central carbon metabolism reacting deterministically. Interestingly, there are some reports of heterogeneity in certain substrate uptake pathways (Acar et al., 2005; Ozbudak et al., 2004). Recently, Solopova et al. found that only part of a *Lactococcus lactis* population continues growth on the second carbon source and proposes that this is a risk-spreading strategy (Solopova et al., 2014). A similar phenomenon is reported for *E. coli* (Kotte et al., 2014). With *B. subtilis* being known for its multiple survival strategies resulting in phenotypic heterogeneity, the question rises whether *B. subtilis* cells respond heterogeneously to the environmental change during diauxic growth as well. Biochemical processes are subject to random fluctuations (Elowitz et al., 2002; Ozbudak et al., 2002) which are often suppressed. This so-called stochasticity, however, can also be exploited to generate phenotypic variation (Choi et al., 2008; Losick and Desplan, 2008; Ozbudak et al., 2004; Veening et al., 2008a). *Bacillus subtilis* is well known for the many phenotypes it generates within an isogenic population. Examples of this are a competent-, a spore forming-, an exoprotease secreting-, a motile-, and a biofilm producing phenotype (Branda et al., 2001; Dubnau, 1991; Errington, 2003; Kearns and Losick, 2005; Msadek, 1999; Veening et al., 2008a). The phenotypic heterogeneity provides an adaptive solution to changing environments by means of risk spreading (Losick and Desplan, 2008; Rainey et al., 2011; Veening et al., 2008a).

Here, we study the diauxic shift in *B. subtilis* cultures at the single cell level, using time-lapse microscopy. The adaptation from glucose to another carbon source is visualized with GFP fused to the promoters of genes necessary for utilization of the second carbon source. Sugars tested include ribose and cellobiose. Genes for utilization of both carbohydrates are under CCR (Miwa et al., 2000; Tobisch et al., 1997; Yoshida et al., 2001). In compliance with traditional views, *B. subtilis* is found to express genes for uptake and utilization of the second carbohydrate, during the lag phase in all cells, at the same point in time. However, the transcription of genes occurs at different rates in each cell, resulting in heterogeneity.

Results

B. subtilis responds homogeneously during the diauxic shift from glucose to ribose.

A diauxic shift is observed when *B. subtilis* 168 is grown on CDM (de Jong et al., 2011a) supplemented with both glucose (0.1%) and ribose (0.4%) (Fig. 1). Initial exponential growth of the bacterial culture halts at the same optical density at 600 nm (OD_{600}) that is reached when only glucose (0.1%) is present in the medium (Fig. 1). After a lag phase with no apparent growth, the OD_{600} continues to increase.

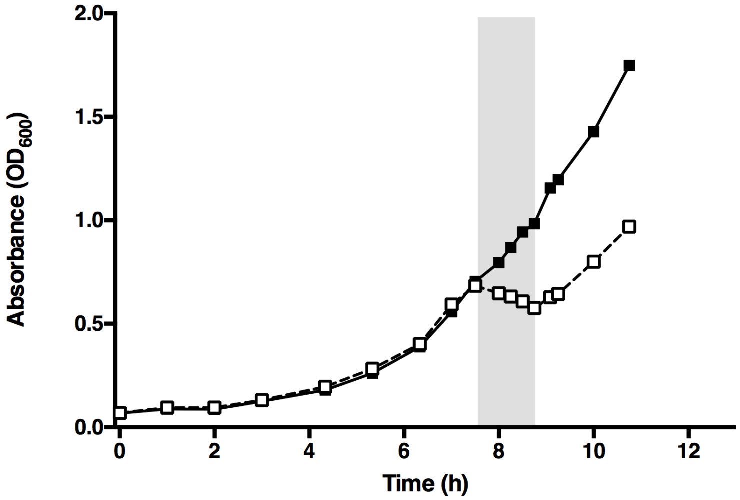

Figure 1. *B. subtilis* diauxic shift. Growth (OD_{600}) of *B. subtilis* in chemically defined medium with 0.5% glucose (■) or a mixture of 0.1% glucose and 0.4% ribose (□). When grown on a mixture of glucose and ribose, cells first consume glucose. After depletion of glucose a lag phase occurs (marked in grey), which is traditionally attributed to required biochemical adaptation for utilization of the second carbohydrate. The second growth phase is on ribose.

For growth on ribose as a sole carbon source, expression of the *rbs* operon is required (Woodson and Devine, 1994). P*rbs* is a promoter of the ribose transport operon, encoding the proteins RbsRKDACB (Woodson and Devine, 1994). P*rbs* was fused to the green fluorescent protein (GFP) in *B. subtilis* 168 *Prbs-gfp* and when cells take up ribose they express GFP.

Using time-lapse microscopy the diauxic shift was studied at the single-cell level (Fig. 2 and Movies S1 and S2). This revealed that cells of an isogenic *B. subtilis* 168 P*rbs-gfp* population grown on a mixture of glucose and ribose all respond to the change in glucose availability by activating P*rbs* (visualized by green fluorescence of GFP). Cells in which P*rbs* is active, express the ribose transporter and kinase, and are able to import ribose, metabolize it and grow. Growth occurred in two phases separated by a lag phase, during which the cells became fluorescent. The initiation of fluorescence seems to occur at the same point in time for all cells. There is some variation between cells in fluorescence intensity, but clearly all cells become fluorescent. During growth on ribose the cells that form spores at a later stage, stop expression of *rbs* genes.

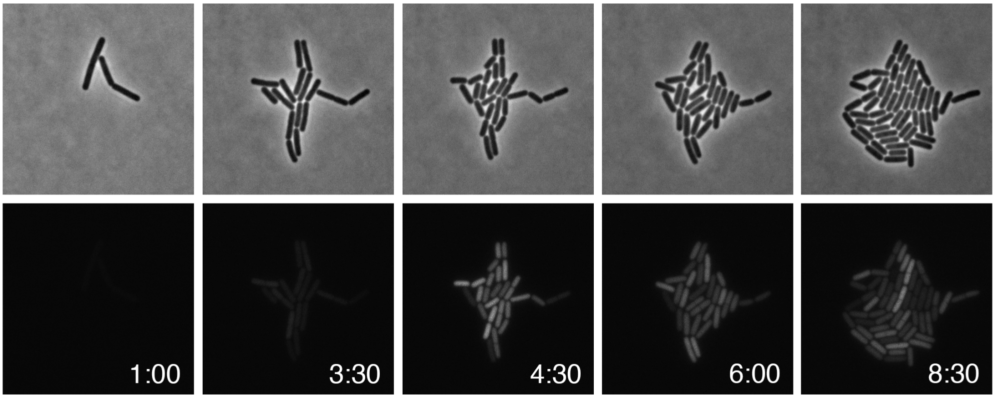

Figure 2. *B. subtilis* diauxic time-lapse experiment. Phase contrast (above) and fluorescence (below) frames of the time-lapse experiment performed in CDM containing glucose and ribose (Movie S1). All cells seemed to be switching to ribose at the same time, while they varied in fluorescence intensity. Time is depicted in hours.

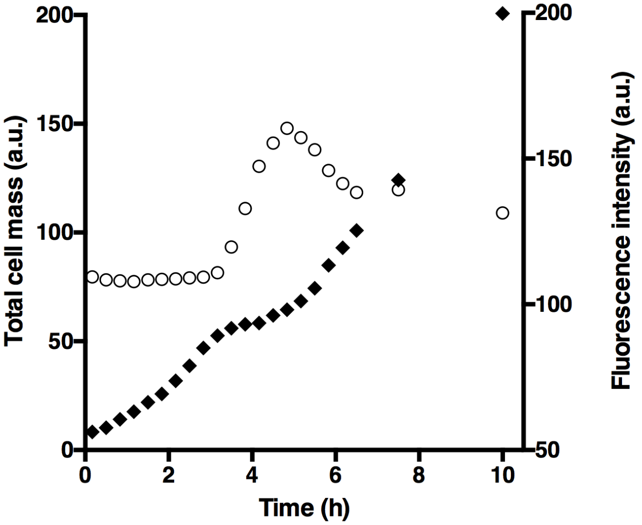

Figure 3. Diauxic shift during time-lapse experiment on glucose and ribose. Quantification of the time-lapse experiment by measuring individual cells illustrates that P*rbs* is activated upon glucose exhaustion and that growth only continues after a lag phase. Data on cell mass (◆) and fluorescence (○) is derived from frames in Movie S1. Only every second measure point has been plotted for better visibility.

For a more precise view on growth and fluorescence during the time-lapse experiment, the total length of all cells and the total fluorescence intensity is measured for each frame (Fig. 3). It becomes clear that the fluorescence increases at the moment that growth has almost stopped. During a short period of no growth the fluorescence continues to increase and when it has almost reached maximum intensity the growth continues. The growth curve from the timelapse experiment (Fig. 3) looks similar to the liquid media growth curve (Fig. 1), displaying typical diauxie. Variations in concentrations of ribose (0.025 - 0.3%) resulted in the same response (results not shown).

Cells exhibited varying levels of fluorescence throughout the time-lapse experiment and to determine whether any obvious subpopulations existed, fluorescence of individual cells was plotted in a histogram (Fig. 4). In general the fluorescence distributions seem unimodal. At time-points 3:30h, 4:30h and 6:00h, a relatively prominent portion of more fluorescent cells is present. At time-point 4:30h, three subpopulations can be observed exhibiting lower, medium and higher fluorescence.

To get a better view of the individual cells' fluorescence and growth over time, single cells present at 2:50h and their offspring later in time were followed. Tracking of both fluorescence intensity and growth of individual cell-lines showed that some cell-lines exhibited a higher fluorescence signal and grew faster than others (Fig. 5). Growth is defined and shown here as total cell length of the cell-line. The onset of transcription (indicated by fluorescence) occurred at the same moment in time for the analysed cell-lines, however, at a different rate (Fig. 5A). This led to variation in timing of the fluorescence peak for each cell-line. Half of the cell-lines reached maximum fluorescence at 4.5h in a synchronized matter, while the other half peaked at varying moments later in time. Regarding cell growth there seems to be an average rate, with some outliers having lower- and higher rates (Fig. 5B). The rate of cell-growth is correlated with the rate of gene transcription.

Although the focus of this chapter lies with ribose, a similar response is also observed during diauxic shift under the same conditions with cellobiose (0.1 - 0.5%) instead of ribose (Fig. S1 & Movie S3).

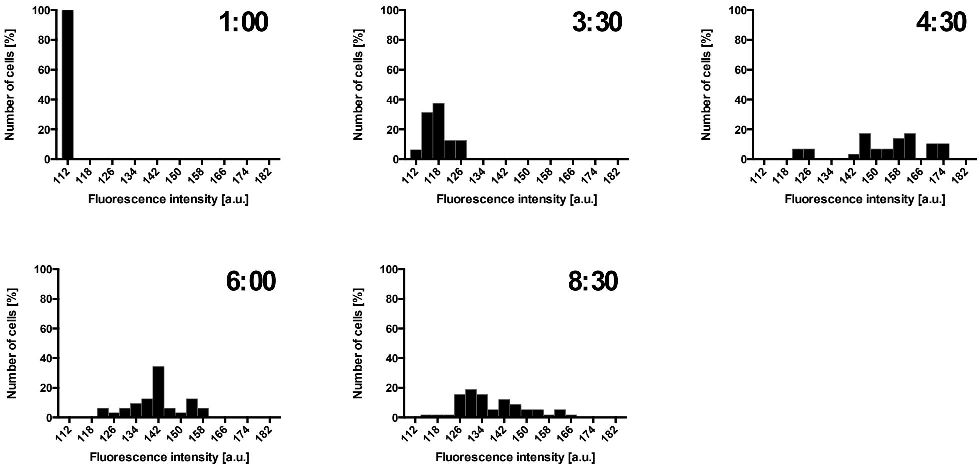

Figure 4. Distribution of fluorescence during diauxic time-lapse experiment. Fluorescence of each individual cell was measured and plotted in a histogram. Shown are the same time-points as in Fig. 2. In general the fluorescence distribution seems to be unimodal. As fluorescence increased over time, the shape of the distribution changed.

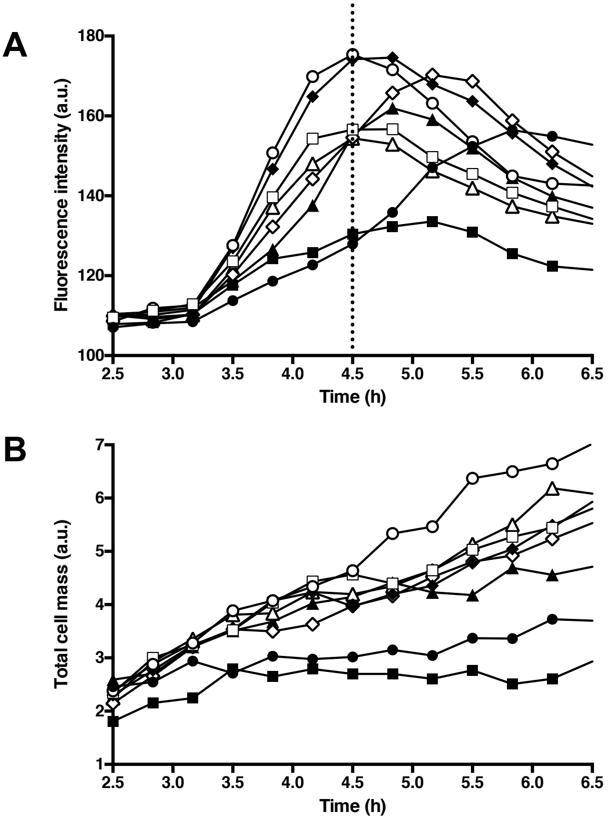

Figure 5. Fluorescence and growth of individual cell lines. Each curve represents a single cell present in the micro-colony at 2.5h and its offspring. Only every second measure point has been plotted for better visibility. **(A)** Fluorescence starts to increase in all cells at the same time. However, the rate of increase varies, resulting in varying moments of peak fluorescence for each cell-line. Half of the cell-lines reach maximum fluorescence at 4.5h in a synchronized matter, while the other half peaks at varying moments later in time. **(B)** There seems to be an average rate of cell-growth, with some outliers having lower- and higher rates. The rate of cell-growth is correlated with the rate of fluorescence increase.

Discussion

Here, we have examined the diauxic shift in *B. subtilis* at the single cell level. This revealed that during this period, the cell population expresses genes required for growth on ribose at the same moment in time, but at a different rate. In compliance with Monod (Monod, 1949), the diauxic lag phase in the *B. subtilis* population growth curve originates from temporal growth arrest of all cells in the population. As visualized by GFP, enzyme synthesis initiates just before the growth on glucose has completely halted (Fig. 2 and 3; Movies S1 and S2). The fact that growth only continues after GFP fluorescence has reached a certain level, suggests that *rbs* expression (and consequently the number of ribose uptake enzymes) is not yet high enough to sustain growth on ribose before glucose is exhausted and that the diauxic lag indeed originates from the time needed for biochemical adaptation.

Recent studies on *L. lactis* (Solopova et al., 2014) and *E. coli* (Kotte et al., 2014) provide an additional explanation for the diauxic lag phase. In these studies a mixed population of cells able and unable to grow on the non-preferred carbon source emerges during the diauxic shift. The culture appears to be non-growing, but actually only a part of the population is contributing to growth. This diversification resulting in a bimodal population spread is possibly a risk-spreading strategy enabling population survival in fluctuating environments (de Jong et al., 2011b; Veening et al., 2008a). The gram-positive *L. lactis* achieves this heterogeneity as follows. The relief of carbon catabolite repression as consequence of glucose depletion enables cells to grow on the second carbohydrate. However, the stringent response activates a protective non-growing state in cells with low energy levels. This results in a fraction of the population able to make the switch to the second carbohydrate and the other fraction of the cells to enter a non-growing state. The fraction size is influenced by the glucose concentration, as higher cell density leads to a more sudden depletion of glucose. In contrast to *B. subtilis* and *L. lactis*, the concentration of the second carbon substrate determines the fraction of adapting *E. coli* cells. In this gram-negative bacteria a principle similar to *L. lactis* is employed, where cells that achieve a sufficiently high metabolic flux on the second carbohydrate are able to grow while the others become dormant (Kotte et al., 2014).

The findings in the studies described above show that global regulatory mechanisms might vary in outcome at the single cell level and that this is highly dependent on the energy state of the cell. That such extreme single cell variations have not been found for carbon utilization in *B. subtilis* under the conditions examined here, does not rule out the possibility for such bimodal heterogeneity during diauxic shift. There are many instances of heterogeneity in differentiating bacteria such as *B. subtilis* (Dubnau, 1991; Elowitz et al., 2002; de Jong et al., 2012; Kearns and Losick, 2005; Losick and Desplan, 2008; Rainey et al., 2011; Veening et al., 2008c) and whether heterogeneity during diauxic growth like reported for *L. lactis* and *E. coli* exists needs to be further elaborated by future experiments under different conditions. The glucose concentrations used in our time-lapse experiments result in significantly less diversification of *L. lactis* cells during diauxic shift than higher glucose concentrations (Solopova et al., 2014). Possibly different concentrations and/or carbohydrates than the ones used in our study may lead to similar responses in *B. subtilis* as in *L. lactis*. It could also be possible that *B. subtilis* simply employs different survival strategies, and instead forms dormant endospores as consequence of diauxic growth. Sporulation is a last resort strategy, delayed as long as possible (González-Pastor et al., 2003) and only visible at the end of the time-lapse experiment. In addition to investigation of single cell response to other carbohydrates and concentrations during diauxic shift, future experiments should determine the influence of the preculture on heterogeneity, since epigenetic mechanisms in determination of cell fate have been described previously (Robert et al., 2010; Solopova et al., 2014; Veening et al., 2008a).

When looking at the microscopy picture (Fig. 2), the fluorescence distribution (Fig. 4), and the individual cell-lines (Fig. 5) of time-point 4:30h, three subpopulations can be observed: low, middle and high fluorescence. The low fluorescence subpopulation is clearly growing at a lower rate. Whether this heterogeneity is present in repeated experiments needs to be found out. Additionally, elaboration of any factors influencing the presence of the subpopulations, like for example cellular aging (Stewart et al., 2005; Veening et al., 2008c) and carbohydrate concentrations (Kotte et al., 2014; Solopova et al., 2014), would be interesting.

Our work acknowledges the paradigm proposed by Monod: under the conditions tested here, a slow/non-growing *B. subtilis* population responsively expresses genes required for growth on the second carbon source at the same moment in time. In contrast to the recent findings on heterogeneity during diauxie in other bacteria (Kotte et al., 2014; Solopova et al., 2014), fractionation into a non-growing subpopulation does not play a role in the *B. subtilis* diauxic lag phase described in this chapter. However, the ribose gene expression during diauxic shift is heterogeneous and a slower growing subpopulation seems to be present that may very well lead to non-growing subpopulations under conditions different from tested here. This can be, for example, a higher glucose concentration, leading to a higher cell density and a more sudden depletion of glucose. Future experiments under varying environmental conditions will have to clarify this.

Material & methods

Bacterial strains, plasmids, media and growth conditions.

Bacterial strains and plasmids used in this study are listed in Table 1. *Bacillus subtilis* was grown with 200 rpm shaking at 37°C in LB (Sambrook et al., 1989) or in chemically defined medium (CDM) (de Jong et al., 2011a) supplemented with glucose, ribose or cellobiose. For growth on solid media, LB solidified with 1.5% (wt/vol) agar was used. For microscopy time-lapse experiments, cells were grown in CDM with glucose (0.05 - 0.5%) until mid-exponential phase was reached, washed with CDM and transferred to a microscopy slide with a 1.5% high-resolution agarose layer with CDM medium (0.005% glucose and varying concentrations of ribose or cellobiose).

Escherichia coli DH5α was used as host for cloning and grown in LB medium at 37°C with shaking or on LB medium solidified with 1.5% (wt/vol) agar. When required, the growth media were supplemented with the following antibiotics: 100 µg ml^{-1} ampicillin (Amp) for *E. coli*, and 5 µg ml^{-1} chloramphenicol (Cm) for *B. subtilis*.

Recombinant DNA techniques and oligonucleotides.

Procedures for DNA isolation, restriction, ligation, agarose gel electrophoresis, and transformation of *E. coli* were performed as described by Sambrook et al. (1989). Plasmid DNA and PCR products were isolated and purified using the High Pure Plasmid Isolation Kit (Roche Applied Science, Mannheim, Germany) according to the manufacturer's instructions. Enzymes were purchased from New England Biolabs (Ipswich, Great Britain) and Fermentas (Vilnius, Lithuania) and used as described by the manufacturer. For PCR amplification, Phusion- and Taq DNA polymerase (Fermentas) were used. *B. subtilis* was transformed as described by (Harwood and Cutting, 1990). Oligonucleotides used in this study are listed in Table 2 and were purchased from Biolegio (Nijmegen, the Netherlands)

Table 1. Bacterial strains and plasmids.

Strains	**Relevant properties**	**Source or reference**
E. coli DH5α	F-, *araD*139, Δ(*ara-leu*)7696, Δ(*lac*)X74, *galU*, *galK*, *hsdR2*, *mcrA*, *mcrB1*, *rspL*	Laboratory stock
B. subtilis		
168	*trpC2*	(Kunst et al., 1997)
168P*rbsR*-GFP	168, P_{rbsR}-*gfpmut1*, Cm^R	This study
168P*licB*-GFP	168, P_{licB}-*gfpmut1*, Cm^R	This study
Plasmids		
pSG1151	*bla, cat, gfpmut1*	(Lewis and Marston, 1999)
pGFP-*rbsR*	*bla, cat,* P_{rbsR}-*gfpmut1*	This study
pGFP-*licB*	*bla, cat,* P_{licB}-*gfpmut1*	This study

Table 2. Oligonucleotides used in this study. Restriction sites are underlined.

Primers	**Sequence (5\` to 3\`)**	**Description; position**
pGFP-R-seq	GTTGGCCATGGAACAGGTAG	5\` end of GFP
P*rbsR*-F+KpnI	GCGCGGTACCAGCAGGACTTATACCTTATC	KpnI; 5\` end of P*rbsR*
P*rbsR*-R+RBS+HindIII	GCGCAAGCTTCATTTCCTCTCCTCCTTATGTAACCGTTTACATAGATAG	HindIII; 3\` end of P*rbsR*
P*licB*-F+HindIII	GCGCGCAAGCTTCAGTACTGAAGGTTAACACC	HindIII; 5\` end of P*licB*
P*licB*-R+RBS+EcoRI	CGGCGGAATTCCATTTCCTCTCCTCCTATTTTGTAATGTCCTGCTGTTG	EcoRI; 3\` end of P*licB*

Construction of plasmids

For construction of the promoter-gfp fusion plasmids, approximately 600-700 bps of the corresponding promoter regions were PCR-amplified using *B. subtilis* 168 chromosomal DNA as template. All known regulatory sequences (http://dbtbs.hgc.jp/) were included. To obtain a stronger GFP signal, the native RBS was replaced with the strong RBS from *wapA* using ATG as a start codon (Veening et al., 2008b). The resulting PCR fragments were ligated in front of the *gfpmut1* gene on plasmid pSG1151 (Lewis and Marston, 1999) via the PstI/HindIII and HindIII/EcoRI restriction sites. The inserted promoter region was checked by sequencing with pGFP-seq-R (GTTGGCCATGGAACAGGTAG).

Construction of strains

B. subtilis strains 168_PrbsR-GFP and 168_PcelB-GFP were obtained by Campbell-type integration of the corresponding promoter-*gfp* fusion plasmids into the native locus on the *B. subtilis* 168 chromosome (Kunst et al., 1997). During this event the wildtype background of the corresponding genes was left intact. Transformants were selected on LB agar plates containing chloramphenicol after overnight incubation at 37°C.

Microscopy

Microscopy images were taken with an Olympus IX71 Microscope (Personal DV, Applied Precision; assembled by Imsol, Preston, UK) using CoolSNAP HQ2 camera (Princeton Instruments, Trenton, USA) with a 100× phase-contrast objective. Fluorescence filter sets (excitation, 450 to 490 nm; emission, 500 to 550 nm) used to visualize GFP were from Chroma Technology Corporation (Bellows Falls, USA). Exposure time was 0.2 s with 32% excitation xenon light (300 W). Softworx 3.6.0 (Applied Precision, Washington, USA) software was used for image capturing. Time-lapse microscopy and preparation of the microscope sample is performed as described in detail by de Jong et al. (2011). ImageJ was used to quantify cell lengths and fluorescence intensities in each frame of the time-lapse movies, as described by de Jong et al. (2011).

Acknowledgements

The PhD project of Wout Overkamp was financed by the Kluyver Centre for Genomics of Industrial Fermentation which is part of the Netherlands Genomics Initiative / Netherlands Organisation for Scientific Research (NWO).

References

Acar, M., Becskei, A., and van Oudenaarden, A. (2005). Enhancement of cellular memory by reducing stochastic transitions. Nature *435*, 228–232.

Branda, S.S., González-Pastor, J.E., Ben-Yehuda, S., Losick, R., and Kolter, R. (2001). Fruiting body formation by *Bacillus subtilis*. Proc. Natl. Acad. Sci. *98*, 11621–11626.

Choi, P.J., Cai, L., Frieda, K., and Xie, X.S. (2008). A stochastic single-molecule event triggers phenotype switching of a bacterial cell. Science *322*, 442–446.

Demoling, F., Figueroa, D., and Bååth, E. (2007). Comparison of factors limiting bacterial growth in different soils. Soil Biol. Biochem. *39*, 2485–2495.

Dubnau, D. (1991). Genetic competence in *Bacillus subtilis*. Microbiol. Rev. *55*, 395–424.

Elowitz, M.B., Levine, A.J., Siggia, E.D., and Swain, P.S. (2002). Stochastic Gene Expression in a Single Cell. Science *297*, 1183–1186.

Errington, J. (2003). Regulation of endospore formation in *Bacillus subtilis*. Nat. Rev. Microbiol. *1*, 117–126.

González-Pastor, J.E., Hobbs, E.C., and Losick, R. (2003). Cannibalism by sporulating bacteria. Science *301*, 510–513.

Harwood, C.R., and Cutting, S.M. (1990). Molecular Biological Methods for *Bacillus* (John Wiley & Sons).

Inada, T., Kimata, K., and Aiba, H. (1996). Mechanism responsible for glucose-lactose diauxie in *Escherichia coli*: challenge to the cAMP model. Genes Cells Devoted Mol. Cell. Mech. *1*, 293–301.

de Jong, I.G., Beilharz, K., Kuipers, O.P., and Veening, J.-W. (2011a). Live Cell Imaging of *Bacillus subtilis* and *Streptococcus pneumoniae* using Automated Time-lapse Microscopy. J. Vis. Exp. JoVE.

de Jong, I.G., Haccou, P., and Kuipers, O.P. (2011b). Bet hedging or not? A guide to proper classification of microbial survival strategies. BioEssays *33*, 215–223.

de Jong, I.G., Veening, J.-W., and Kuipers, O.P. (2012). Single cell analysis of gene expression patterns during carbon starvation in *Bacillus subtilis* reveals large phenotypic variation. Environ. Microbiol. *14*, 3110–3121.

Kearns, D.B., and Losick, R. (2005). Cell population heterogeneity during growth of *Bacillus subtilis*. Genes Dev. *19*, 3083–3094.

Koch, A.L. (1971). The adaptive responses of *Escherichia coli* to a feast and famine existence. Adv. Microb. Physiol. *6*, 147–217.

Kotte, O., Volkmer, B., Radzikowski, J.L., and Heinemann, M. (2014). Phenotypic bistability in *Escherichia coli*'s central carbon metabolism. Mol. Syst. Biol. *10*, 736.

Kunst, F., Ogasawara, N., Moszer, I., Albertini, A.M., Alloni, G., Azevedo, V., Bertero, M.G., Bessières, P., Bolotin, A., Borchert, S., et al. (1997). The complete genome sequence of the gram-positive bacterium *Bacillus subtilis*. Nature *390*, 249–256.

Lewis, P.J., and Marston, A.L. (1999). GFP vectors for controlled expression and dual labelling of protein fusions in *Bacillus subtilis*. Gene *227*, 101–109.

Losick, R., and Desplan, C. (2008). Stochasticity and cell fate. Science *320*, 65–68.

Miwa, Y., Nakata, A., Ogiwara, A., Yamamoto, M., and Fujita, Y. (2000). Evaluation and characterization of catabolite-responsive elements (cre) of *Bacillus subtilis*. Nucleic Acids Res. *28*, 1206–1210.

Monod, J. (1949). The Growth of Bacterial Cultures. Annu. Rev. Microbiol. *3*, 371–394.

Msadek, T. (1999). When the going gets tough: survival strategies and environmental signaling networks in *Bacillus subtilis*. Trends Microbiol. *7*, 201–207.

Ozbudak, E.M., Thattai, M., Kurtser, I., Grossman, A.D., and van Oudenaarden, A. (2002). Regulation of noise in the expression of a single gene. Nat. Genet. *31*, 69–73.

Ozbudak, E.M., Thattai, M., Lim, H.N., Shraiman, B.I., and Van Oudenaarden, A. (2004). Multistability in the lactose utilization network of *Escherichia coli*. Nature *427*, 737–740.

Rainey, P.B., Beaumont, H.J.E., Ferguson, G.C., Gallie, J., Kost, C., Libby, E., and Zhang, X.-X. (2011). The evolutionary emergence of stochastic phenotype switching in bacteria. Microb. Cell Factories *10 Suppl 1*, S14.

Robert, L., Paul, G., Chen, Y., Taddei, F., Baigl, D., and Lindner, A.B. (2010). Predispositions and epigenetic inheritance in the *Escherichia coli* lactose operon bistable switch. Mol. Syst. Biol. *6*, 357.

Sambrook, J., Fritsch, E.F., and Maniatis, T. (1989). Molecular cloning: a laboratory manual (Cold Spring Harbor Laboratory).

Solopova, A., van Gestel, J., Weissing, F.J., Bachmann, H., Teusink, B., Kok, J., and Kuipers, O.P. (2014). Bet-hedging during bacterial diauxic shift. Proc. Natl. Acad. Sci. U. S. A. *111*, 7427–7432.

Stanier, R.Y. (1951). Enzymatic adaptation in bacteria. Annu. Rev. Microbiol. *5*, 35–56.

Stewart, E.J., Madden, R., Paul, G., and Taddei, F. (2005). Aging and death in an organism that reproduces by morphologically symmetric division. PLoS Biol. *3*, e45.

Stülke, J., and Hillen, W. (1999). Carbon catabolite repression in bacteria. Curr. Opin. Microbiol. *2*, 195–201.

Tobisch, S., Glaser, P., Krüger, S., and Hecker, M. (1997). Identification and characterization of a new beta-glucoside utilization system in *Bacillus subtilis*. J. Bacteriol. *179*, 496–506.

Veening, J.-W., Smits, W.K., and Kuipers, O.P. (2008a). Bistability, epigenetics, and bet-hedging in bacteria. Annu. Rev. Microbiol. *62*, 193–210.

Veening, J.-W., Igoshin, O.A., Eijlander, R.T., Nijland, R., Hamoen, L.W., and Kuipers, O.P. (2008b). Transient heterogeneity in extracellular protease production by *Bacillus subtilis*. Mol. Syst. Biol. *4*, 184.

Veening, J.-W., Stewart, E.J., Berngruber, T.W., Taddei, F., Kuipers, O.P., and Hamoen, L.W. (2008c). Bet-hedging and epigenetic inheritance in bacterial cell development. Proc. Natl. Acad. Sci. U. S. A. *105*, 4393–4398.

Woodson, K., and Devine, K.M. (1994). Analysis of a ribose transport operon from *Bacillus subtilis*. Microbiology *140*, 1829–1838.

Yoshida, K., Kobayashi, K., Miwa, Y., Kang, C.-M., Matsunaga, M., Yamaguchi, H., Tojo, S., Yamamoto, M., Nishi, R., Ogasawara, N., et al. (2001). Combined transcriptome and proteome analysis as a powerful approach to study genes under glucose repression in *Bacillus subtilis*. Nucleic Acids Res. *29*, 683–692.

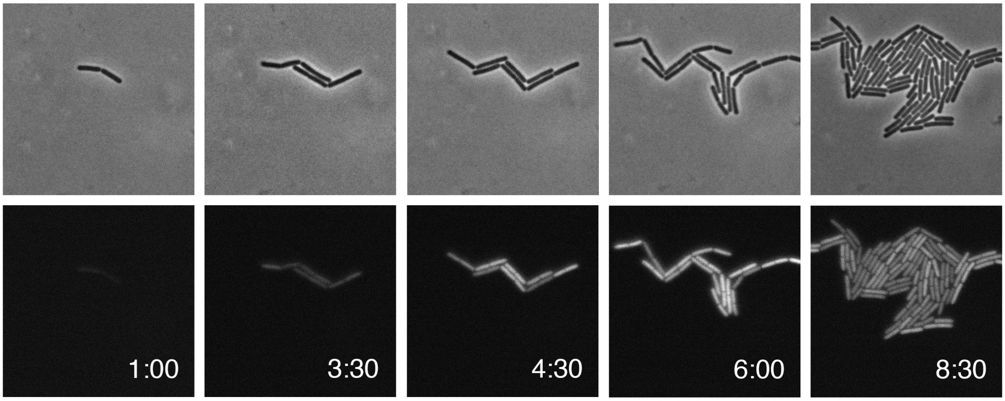

Figure S1. ***B. subtilis*** **diauxic time-lapse experiment on cellobiose.** Phase contrast (above) and fluorescence (below) frames of the time-lapse experiment performed in CDM containing 0.05% glucose and 0.1% cellobiose (Movie S3). For growth on cellobiose as a sole carbon source, expression of the *lic* operon is required (Tobisch et al., 1997). P*lic* is a promoter of the cellobiose transport operon, encoding the proteins LicBCAH. P*lic* was fused to the green fluorescent protein (GFP) in *B. subtilis* 168 *Plic-gfp* and when cells take up cellobiose they express GFP. All cells switch to cellobiose at the same time, illustrating a response that is similar to the ribose diauxic shift. In Movie S3, the lag phase is much less pronounced than on ribose. Time is depicted in hours.